



HAL
open science

Charging of heated colloidal particles using the electrolyte Seebeck effect

Arghya Majee, Alois Würger

► **To cite this version:**

Arghya Majee, Alois Würger. Charging of heated colloidal particles using the electrolyte Seebeck effect. *Physical Review Letters*, 2012, 108 (11), pp.118301. 10.1103/PhysRevLett.108.118301. hal-00678357

HAL Id: hal-00678357

<https://hal.science/hal-00678357>

Submitted on 12 Mar 2012

HAL is a multi-disciplinary open access archive for the deposit and dissemination of scientific research documents, whether they are published or not. The documents may come from teaching and research institutions in France or abroad, or from public or private research centers.

L'archive ouverte pluridisciplinaire **HAL**, est destinée au dépôt et à la diffusion de documents scientifiques de niveau recherche, publiés ou non, émanant des établissements d'enseignement et de recherche français ou étrangers, des laboratoires publics ou privés.

Charging of heated colloidal particles using the electrolyte Seebeck effect

Arghya Majee and Alois Würger

*Laboratoire Ondes et Matière d'Aquitaine, Université de Bordeaux & CNRS,
351 cours de la Libération, 33405 Talence, France*

We propose a novel actuation mechanism for colloids, which is based on the Seebeck effect of the electrolyte solution: Laser heating of a nonionic particle accumulates in its vicinity a net charge Q , which is proportional to the excess temperature at the particle surface. The corresponding long-range thermoelectric field $E \propto 1/r^2$ provides a tool for controlled interactions with nearby beads or with additional molecular solutes. An external field E_{ext} drags the thermocharged particle at a velocity that depends on its size and absorption properties; the latter point could be particularly relevant for separating carbon nanotubes according to their electronic bandstructure.

PACS numbers:

Selective transport and controlled pattern formation are of fundamental interest in microfluidics and biotechnology [1]. Particle focussing devices [2–4] and macromolecular traps [5–7] have been designed by applying chemical or thermal gradients. In “active colloids” there is no external symmetry breaking field: Thermodynamic forces arise from an embarked chemical reactor [8, 9] or from non-uniform laser heating of Janus particles [10]. In both cases the colloid self-propels in an anisotropic environment that is created by the concentration or temperature variation along its surface. The interplay of self-propulsion and Brownian motion leads to a complex diffusion behavior [8–11].

Locally modifying material properties by heating a single nanoparticle or molecule in a focussed laser beam is by now a standard technique. The temperature dependent refractive index was used for the photothermal detection of a single non-fluorescent chromophore [12]. Heating a spherical nanoparticle induces a radial temperature profile in the surrounding fluid and, because of the viscosity change, an enhancement of the Einstein coefficient [13]. The non-uniform laser absorption of half-metal coated particles leads to a temperature variation along its surface; the resulting self-propulsion adds a ballistic velocity component and thus increases the effective mean-square displacement [10].

In this Letter, we point out that heating confers a net charge on colloidal particles, and how this electrolyte Seebeck effect in the vicinity of a heated bead can be used for selective transport and controlled interactions. After a brief reminder of the well-known case of a constant temperature gradient, we derive the expressions for the thermocharge and the electric field induced by a spherical particle with excess temperature δT . As possible applications, we then discuss the thermoelectric pair potential, aggregation or depletion of a molecular solute in the vicinity of a hot particle, and colloidal separation through velocity differentiation.

The response of a salt solution to a constant thermal gradient ∇T is illustrated in the left panel of Fig. 1. Because of their temperature dependent solvation energy, positive and negative salt ions migrate along the gradient. In general one of the species moves more rapidly,

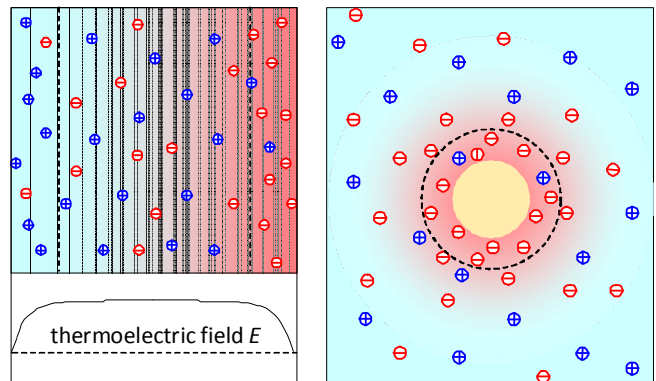


FIG. 1: Left panel: Seebeck effect in an electrolyte solution that is cooled at the left side and heated at the right. We show the case of a positive Seebeck coefficient S , where cations and anions accumulate at the cold and hot boundaries, respectively. These charged layers have a thickness of about one Debye length (dashed lines). The corresponding thermoelectric field E is constant in the bulk and vanishes at the boundaries [20]. Right panel: Seebeck effect in the vicinity of a hot particle with excess temperature δT . Due to the radial temperature gradient, a net charge Q accumulates within one Debye length from the particle surface. The charge density and the radial electric field are shown in Fig. 2 below. The counterions are at the vessel boundary.

resulting in a thermopotential between the cold and hot boundaries of the sample [14] and a macroscopic electric field $E = S\nabla T$, which is proportional to the thermal gradient and to the Seebeck coefficient S [15]. The bulk solution is neutral; yet opposite charges accumulate at the boundaries and screen the electric field in a layer of one Debye length. In the last years it has become clear that charged colloids in a temperature gradient are a sensitive probe to the Seebeck effect of the electrolyte solution [16, 17]: The field E and thus the colloidal velocity depend strongly on the salt composition and are particularly important in the presence of molecular ions containing hydrogen [18–20]; this thermo-electrophoretic driving has been confirmed for SDS micelles in a $\text{NaCl}_{1-x}\text{OH}_x$ solution, where a change of sign of the drift velocity has

been observed upon varying the parameter x [17].

Thermocharge of a hot colloid. Now we consider the Seebeck effect in the vicinity of a heated particle, as shown in the right panel of Fig. 1. The qualitative features are readily obtained by wrapping the hot boundary of the one-dimensional case (left panel) onto a sphere of radius a . Its excess temperature δT results in a thermal gradient

$$\nabla T = -\frac{\delta T a}{r^2} \quad (1)$$

and, at distances well beyond the Debye length, in a thermoelectric field $E = S\nabla T$. Its complete expression, in particular close to the particle surface, is obtained from the stationary electro-osmotic equations for the ion currents

$$J_{\pm} = -D_{\pm} \left(\nabla n_{\pm} \mp n_{\pm} \frac{eE}{k_B T} + 2n_{\pm} \alpha_{\pm} \frac{\nabla T}{T} \right), \quad (2)$$

which comprise normal diffusion with coefficients D_{\pm} , electrophoresis with the Hückel mobility for monovalent ions, and thermal diffusion with parameters α_{\pm} . The latter are reduced values of the ionic Soret coefficient, introduced by Eastman as a measure for the electromotive force of an electrolyte thermocouple [14]; experimental values are found in Refs. [15, 21, 22].

The thermoelectric field E and the charge density $\rho = e(n_+ - n_-)$ are obtained from the steady-state condition $J_{\pm} = 0$ and Gauss' law $\text{div} E = \rho/\epsilon$. Linearizing the currents in the small gradients and solving the coupled differential equations for E and ρ , we obtain the radial steady-state thermoelectric field

$$E = S\nabla T \left(1 - \frac{r + \lambda}{a + \lambda} e^{(a-r)/\lambda} \right), \quad (3)$$

with the Debye length λ and the Seebeck coefficient $S = (\alpha_+ - \alpha_-)k_B/e$. For a detailed calculation see Ref. [23]. With (1) the field E is zero on the particle surface and at infinity, as required by electrostatic boundary conditions. At distances well beyond λ the exponential factor vanishes; the remaining long-range contribution $E = S\nabla T$ varies with the inverse square of the distance r . From Gauss' law one obtains the charge density [23]

$$\rho = \frac{Q e^{(a-r)/\lambda}}{4\pi(a + \lambda)\lambda r},$$

which is concentrated within about one Debye length from the particle surface. Fig. 2 illustrates the variation of E and ρ with distance for different values of λ ; the former is long-range whereas the latter decays exponentially. The net thermocharge carried by an otherwise non-ionic particle,

$$Q = -e(\alpha_+ - \alpha_-) \frac{a}{\ell_B} \frac{\delta T}{T}, \quad (4)$$

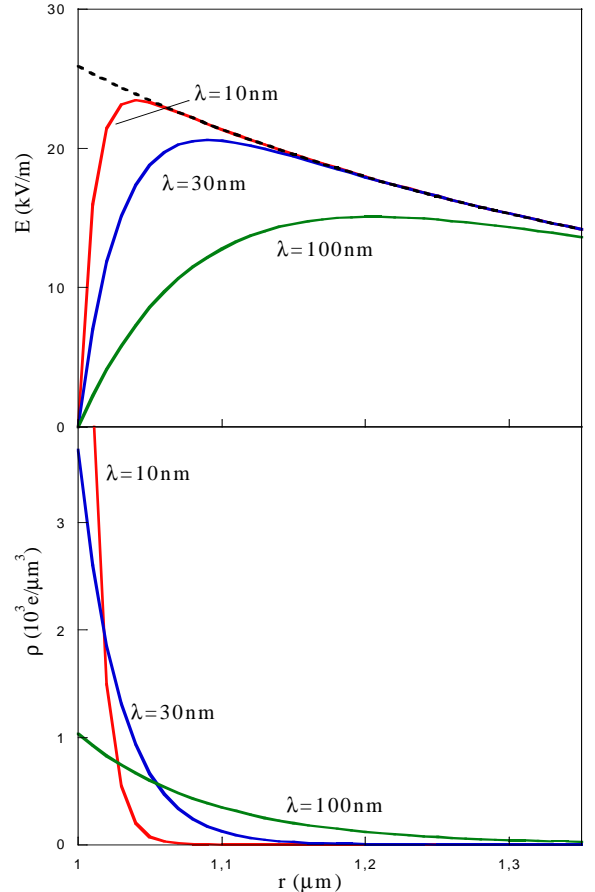


FIG. 2: Thermoelectric field E and charge density ρ as a function of the distance r from the particle centre for different values of the Debye length λ and fixed particle size $a = 1\mu\text{m}$. We have used the parameters $\alpha_+ - \alpha_- = -10$ and $\delta T = 30$ K. The dashed line gives the bulk law $E = S\nabla T$.

depends on its radius in units of the Bjerrum length $\ell_B = 7 \text{ \AA}$, the ratio of excess and absolute temperature, and the reduced Seebeck parameter $\alpha_+ - \alpha_-$ [19].

In physical terms the charge Q arises from the difference in thermo-osmotic pressure of positive and negative ions, which in turn is related to the ionic Soret parameters α_{\pm}/T [14]. For $\alpha_+ > \alpha_-$ the anions show thermal diffusion toward higher temperature, thus accumulating a negative charge at the particle surface. The corresponding cations are located at $r \rightarrow \infty$; in the case of a spherical sample container of radius R , the corresponding surface charge density $Q/4\pi R^2$ is very small. Numerical values for the Seebeck coefficient of several electrolytes are given in Table 1. For small ions the numbers α_{\pm} are of the order of unity; higher values occur for molecules containing hydrogen. For a 100 nm-bead in NaOH or HCl solution with $\delta T = 30$ K, one finds that Q corresponds to about 40 elementary charges; still higher

TABLE I: Seebeck coefficient S for NaCl, HCl and NaOH in aqueous solution [15, 21], and for tetrabutylammonium nitrate (TBAN) in water (w) and dodecanol (d) [22]. For comparison, S of simple metals is of the order of a few $\mu\text{V}/\text{K}$. The Seebeck coefficient is related to Eastman's ionic entropy of transfer $2k_B\alpha_{\pm}$ through $S = (k_B/e)(\alpha_+ - \alpha_-)$ [19]. Experimental values for various ions are given in Refs. [14, 15, 21, 22].

Salt/solvent	NaCl/w	NaOH/w	HCl/w	TBAN/w	TBAN/d
S (mV/K)	0.05	-0.22	0.21	1.0	7.2
$\alpha_+ - \alpha_-$	0.6	-2.7	2.6	12	86

values occur for protonated salts.

Equations (3) and (4) are the main formal results of this paper. In the remainder we discuss how the thermocharge allows to actuate colloidal motility and interactions, and how the thermoelectric field can be used for locally accumulating or depleting an additional charged molecular solute. As an overall feature we estimate the thermoelectric response time. Because of the fast equilibration of heat flow and temperature, thermocharging occurs on the time scale of thermal diffusion of salt ions over one Debye length. With the above parameters one finds a relaxation time of the order of microseconds. Thus on the scale of colloidal motion, thermocharging is an almost instantaneous process.

Colloid-colloid forces. We start with the electric force QE between two hot particles at a distance R . Assuming $R \gg \lambda$ and using the definition of the Bjerrum length, we find

$$F = \frac{Q^2}{4\pi\epsilon R^2}. \quad (5)$$

Thus in an electrolyte with finite Seebeck coefficient, heating disperses colloidal aggregates and strongly affects collective effects due to thermophoretic or hydrodynamic interactions [24]. So far we have considered non-ionic colloids. A particle carrying a proper charge Q_p gives rise to an additional electric field $E_p = Q_p e^{-(r-a)/\lambda} / (4\pi\epsilon\lambda r)$. Depending on the sign of Q and Q_p , the superposition $E + E_p$ shows a complex spatial variation; note that E_p is screened whereas E is not.

Thermo-electrophoresis. Thermocharging provides a unique tool for creating a radial electric field in an electrolyte solution. For a micron-size bead with an excess temperature $\delta T = 30$ K, the field E may attain 10^4 V/m in its immediate vicinity, and a few V/m at a distance of 100 microns. The electrophoretic velocity of a molecular solute with zeta potential ζ ,

$$u = \frac{2}{3} \frac{\epsilon\zeta}{\eta} E, \quad (6)$$

varies between 10 $\mu\text{m}/\text{s}$ and 10 nm/s . Depending on the sign of the zeta potential ζ and of the Seebeck coefficient, molecular ions are attracted or repelled by the thermocharge. As illustrated in Fig. 3a., this can be used

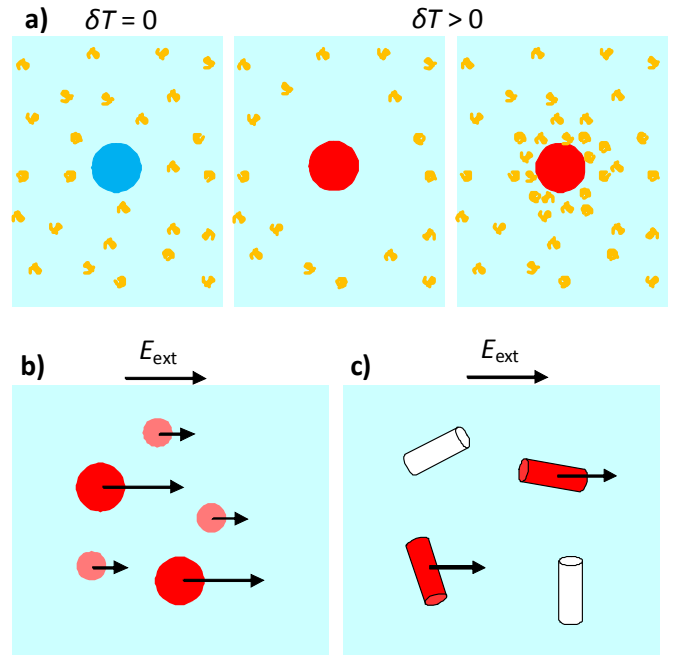


FIG. 3: Pattern formation and selective transport due to thermocharging. a) The thermoelectric field of a hot particle induces electrophoretic motion (6) of a charged molecular solute. Depending on the sign of the electrolyte Seebeck coefficient S and the molecular zeta potential ζ , the colloidal thermocharge results in depletion or accumulation of the solute. b) In an external electric field E_{ext} , heated particles with excess temperature δT and thermocharge Q , acquire a size-dependent velocity (7). c) Because of their different optical absorption properties, metallic and semiconducting carbon nanotubes differ in their thermocharge and in their response to an electric field.

for accumulating or depleting a molecular solute in the vicinity of the particle.

More complex patterns are realized by superposing E with the screened field E_p of a proper charge. In addition to thermo-electrophoresis (6), the radial temperature profile results in thermal diffusion of the solute molecules, due to both double-layer and dispersion forces [19, 25]. Finally we mention that the thermoelectric field E of Janus particles comprises a strongly anisotropic short-range component.

Selective transport. Sorting molecular or colloidal solutes by size is of interest for various applications. The sedimentation potential being rather ineffective for submicron particles, common methods are based on electrophoresis or on motion driven by thermodynamic forces. Since the free-solution mobilities are in general independent of size and molecular weight, velocity differentiation is achieved only after adding a molecular solute as in gel electrophoresis [26, 27], or by spatial flow or field modulation [28–30].

Here we show that thermocharging in the presence of an applied electric field E_{ext} , provides an efficient means

for separating particles by size. The force density ρE_{ext} exerted by the external field on the charged fluid results in a drift velocity u_{ext} of the particle; solving the stationary Stokes equation one finds [23]

$$u_{\text{ext}} = \frac{QE_{\text{ext}}}{6\pi\eta(a + \lambda)}. \quad (7)$$

Note the explicit dependence on the particle size, in contrast to the Helmholtz-Smoluchowski mobility. In view of the thermocharge (4), the most interesting dependencies arise from the excess temperature δT . Assuming a constant volume absorption coefficient β , one finds that the excess temperature varies with the square of the radius,

$$\delta T = \frac{a^2\beta I}{3\kappa}, \quad (8)$$

where I is the laser intensity and κ the thermal conductivity of the solvent.

According to (8) the excess temperature increases with the square of the bead size; thus the drift velocity u_{ext} varies with the particle surface in the Hückel limit ($a < \lambda$) and with its volume in the case $a > \lambda$, as illustrated in Fig. 3b. As an order-of-magnitude estimate, heating the beads by $\delta T = 30$ K and applying a field $E_{\text{app}} \sim 10^4$ V/m results in a velocity of about $10 \mu\text{m/s}$. The above argument holds true for non-spherical solute particles, albeit

with different geometrical factors. The excess temperature of metal-coated polystyrene beads is linear in the radius. For polymers the charge Q is proportional to the chain length or number N of monomers, whereas the friction coefficient varies with the gyration radius $R \propto N^\nu$, resulting in a velocity $u \propto N^{1-\nu}$. In aqueous solution most colloids carry a proper charge with surface potential ζ_p , resulting in an additional velocity $u_p = (\varepsilon\zeta_p/\eta)E_{\text{ext}}$. Still, the thermocharge leads to a significant dispersion of the total velocity $u_{\text{ext}} + u_p$.

We conclude with a possible application to the separation of carbon nanotubes by their wrapping structure [29, 31]. The electronic and optical properties of single-wall nanotubes depend crucially on their ‘‘chiral vector’’ (n, m) that describes the orientation of the graphene structure with respect to the tube axis. Depending on these indices, one has metallic or semiconducting nanotubes with a characteristic bandstructure and a particular optical spectrum. The excess temperature $\delta T = a\bar{\beta}I/\kappa$ of a nanotube depends on its radius a and the absorption per unit area $\bar{\beta}$ of its graphene sheet, and so does the drift velocity u_{ext} . As illustrated in Fig. 3c, by choosing an appropriate laser wave length, one could selectively heat nanotubes with a given chiral vector and separate them through thermocharge electrophoresis.

-
- [1] T.M. Squires, S.R. Quake, *Rev. Mod. Phys.* **77**, 977 (2005)
- [2] B. Abécassis et al., *Nature Mater.* **7**, 785 (2008)
- [3] D. C. Prieve, *Nature Mater.* **7**, 769 (2008)
- [4] J. Palacci, C. Cottin-Bizonne, C. Ybert, and L. Bocquet, *Phys. Rev. Lett.* **105**, 088304 (2010)
- [5] S. Duhr, D. Braun, *Phys. Rev. Lett.* **97**, 038103 (2006)
- [6] H.-R. Jiang, H. Wada, N. Yoshinaga, M. Sano, *Phys. Rev. Lett.* **102**, 208301 (2009)
- [7] C.J. Wienken, Ph. Baaske, U. Rothbauer, D. Braun, S. Duhr, *Nature Communications* **1**, 100 (2010)
- [8] R. Golestanian, T.B. Liverpool, A. Ajdari, *Phys. Rev. Lett.* **94**, 220801 (2005)
- [9] J.R. Howse et al., *Phys. Rev. Lett.* **99**, 048102 (2007)
- [10] H.-R. Jiang, N. Yoshinaga, M. Sano, *Phys. Rev. Lett.* **105**, 268302 (2010)
- [11] R. Golestanian, *Phys. Rev. Lett.* **102**, 188305 (2009)
- [12] A. Gaiduk, M. Yorulmaz, P.V. Ruijgrok, M. Orrit, *Science* **330**, 353 (2010)
- [13] D. Rings, R. Schachoff, M. Selmke, F. Cichos, K. Kroy, *Phys. Rev. Lett.* **105**, 090604 (2010)
- [14] E.D. Eastman, *J. Am. Chem. Soc.* **50**, 283 and 292 (1928)
- [15] J.N. Agar et al., *J. Phys. Chem.* **93**, 2082 (1989)
- [16] S.A. Putnam, D.G. Cahill., *Langmuir* **21**, 5317 (2005)
- [17] D. Vigolo, S. Buzzaccaro, R. Piazza, *Langmuir* **26**, 7792 (2010)
- [18] A. Würger, *Phys. Rev. Lett.* **101**, 108302 (2008).
- [19] A. Würger, *Rep. Prog. Phys.* **73**, 126601 (2010)
- [20] A. Majee, A. Würger, *Phys. Rev. E* **83**, 061403 (2011).
- [21] V.N. Sokolov, L. P. Safonova, A.A. Pribochenko, *J. Solution Chem.* **35**, 1621 (2006)
- [22] M. Bonetti, S. Nakamae, M. Roger, P. Guenoun, *J. Chem. Phys.* **134**, 114513 (2011)
- [23] See Supplemental Material for a detailed calculation of the quantities E , Q , and u_{ext} .
- [24] R. Golestanian, arXiv:1110.1603 (2011)
- [25] R. Piazza, *Soft Matter* **4**, 1740 (2008)
- [26] E.M. Southern, R. Anand, W.R.A. Brown, D.S. Fletcher, *Nucl. Acids Res.* **15**, 5925 (1987)
- [27] J.L. Viovy, *Rev. Mod. Phys.* **72**, 813 (2000)
- [28] J. Han, H. G. Craighead, *Science* **288**, 1026 (2000)
- [29] M. Zheng, A. Jagota, E.D. Semke, B.A. Diner, R.S. Mclean, S.R. Lustig, R.E. Richardson, N.G. Tassi, *Nature Mat.* **2**, 338 (2003)
- [30] L.R. Huang, E.C. Cox, R.H. Austin, J.C. Sturm, *Science* **304**, 987 (2004)
- [31] M.S. Arnold et al., *Nature Nanotechnology* **1**, 60 (2006)